Journal of Materials, Processing and Design (2022)
Clausius Scientific Press, Canada

DOI: 10.23977/jmpd.2022.060109
ISSN 2516-0923 Vol. 6 Num. 1

A New Method to Improve the Mechanism Model of Carburizing by Multivariate Linear Regression

Xinbo Gao[1], Xiaoxu Chen[1], Qiqi Li[1,*]

[1]China Academy of Information and Communications Technology, Beijing, China
**Corresponding author*

Keywords: Machine learning, carburization, Heat treatment

Abstract: Heat treatment is one of the essential technologies in industrial manufacturing, and carburization is one of the processes of heat-treatment technology. With the increase of the technological requirements of production, the optimization of carburizing technology is desired. However, most carburization mechanism models are derived from the material properties and the related physical principles, which are involved huge amounts of parameters. Some parameters (such as diffusion constant, thermal conductivity, interface transfer coefficient, etc.) are difficult to measure correctly, and this is an extremely unfavorable issue to cause the results of the mechanism model inaccurate. In this paper, a new method is raised to improve the carburization mechanism model. The function of the method is to reduce the error of the model results by combining the mechanism model and the multivariate linear regression model with a small amount of sample data. At last, the author of this paper will perform experiments to prove the correctness of the method.

1. Introduction

1.1. The applications of the mechanism model in heat-treatment

Heat-treatment is a technology to change the internal structure of solid material by heating, heat preservation, and cooling, which is usually used to make the interior of the workpiece transfer to the expected structure and performance [1]. Carburization is a key process of heat-treatment, which is to heat the workpiece in the carbon potential medium and transfer the workpiece to an austenite state, then make the workpieces form an enriched carbon layer on the surface [2, 3]. After quenching and low-temperature tempering, the surface layer of the workpiece presents the characteristics of high hardness and wear resistance, and the center of the workpiece has still maintained the toughness and plasticity of low carbon steel [4].

With the gradual increase in technology requirements, the predictions of carburized layer depth and carbon concentrations are necessary. Although the carburizing process models have been maturely researched, many scholars have carried out a variety of models to explore the relationship between the input variables and the effects of the materials after carburizing process [5–7]. However, most carburization mechanism models are derived from the material's characteristics and the physical principles, which involved huge amounts of parameters. Some parameters (such as diffusion constant, thermal conductivity, interface transfer coefficient, etc.) are arduous to measure correctly, which is

an unfavorable issue to cause the results of the mechanism model inaccurate [5, 7]. Therefore, to ensure the accuracy of the model results, a new method is raised to improve the carburization mechanism model in this paper. The function of the method is to reduce the error of the model results by combining the mechanism model and the multivariate linear regression model with a small amount of sample data.

1.2. The applications of machine learning in the carburization mechanism model

Machine learning is a widely used prediction model. The features of the machine learning model are high accuracy, simple structure, high efficiency, strong robustness, and so on. Machine learning includes linear regression model, logical regression model, support vector machine model, k-nearest neighbor model, naive Bayes model, etc [8]. Among those models, the multivariate linear regression (MLR) model has been provided with the function of making the most accurate prediction by minimizing the model error [8, 9], which resolves the pain point of the workpiece carburization mechanism model. Therefore, the author of this paper uses the MLR model of machine learning as the basis to explore the method of optimizing the carburization mechanism model.

2. Experiment set up and model

2.1. Materials, parameters, and Experiment set up

The materials of workpieces for carburizing process are generally low carbon steel or low carbon alloy steel (carbon concentration is less than 0.25%). The material composition parameters used in the experiments are shown in Appendix A.

2.1.1. Process parameters set up

The device parameters set up:
Time of carburizing process (t): 8 hours
The temperature of carburizing process (T): 850 920 950 ℃
0Carburizing potential (C_p): 1.2%
Interface transfer coefficient [4]:

$$\beta = 0.437 * \mathrm{e}^{(-\frac{79953}{RT})} \tag{1}$$

In the equation, R is the ideal gas constant ($R = 8.314\ \mathrm{J/k*mol}$), and T is the temperature of the carburizing process (K).

Diffusion coefficient [4]:

$$D = D_o * e^{(-\frac{Q}{RT})} \tag{2}$$

In the equation, D_o is the Diffusion constant ($D_o = 16.2\ \mathrm{mm^2}/s$ in austenite), and Q is the Diffusion activation energy of carbon ($Q = 137800\ \mathrm{J/mol}$).

2.1.2. Experiment set up

Carburizing experiments were carried out in professional heat-treatment equipment (Fengdong BBH-600-2R). The details of the equipment are shown in Table 1. The picture of the equipment is shown in Fig. 1.

Table 1: The details of the heat-treatment equipment

Type	BBH-600-2R
Effective Dimensions (mm)	600*600*1200
Treating Capacity (KG/Lot)	600
Working Temperature	800-950
Heating Power (KW)	90
Gas Heating Power (KW)	150

Figure 1: The picture of the heat-treatment equipment

The experiments were performed 3 times, each time at a different temperature, as the 850 920 950 ℃. A total of 33 different materials were prepared, and 30 cylindrical samples were made from each material. In every experiment, 10 cylindrical samples of each material are put inside the furnace to heat for 8 hours, then taken out and cut according to the cylindrical axis. After cutting, a heat treatment carburizing calibration analyzer (Huamin hm-bx-3g) was used to analyze the carbon concentration of the cross-section of the product and recorded the carbon concentration for each sample as experimental data. Fig.2 shows the sample for the carburizing experiments.

After 3 experiments, a total of 990 number was recorded in a database, then divided the database into 10 sets. Among the 10 sets of data, 9 sets were used in machine learning for model optimization, and 1 set was used to verify the accuracy of model simulation results.

Figure 2: The samples for the carburizing experiments.

2.2. The mechanism model of carburizing process

2.2.1. The first boundary condition

According to Fick's diffusion law, initial conditions, and the first boundary condition, the equation can be formed as [4],

$$\begin{cases} \frac{\partial C}{\partial t} = D\frac{\partial^2 C}{\partial x^2} & x > 0, t > 0 \\ C(x,0) = C_0 & 0 \le x < \infty,\ t = 0 \\ C_s = C(0,t) = C_p & x = 0, 0 < t < \infty \end{cases} \quad (3)$$

In the equation, C is the carbon concentration (vol%). t is the carburizing time (s). x is the distance between the measuring position and the sample surface (mm). C_s is the carbon concentration on the surface of the product (vol%). C_P is the carbon potential generated by the heat treatment equipment (vol%).

According to equation (3), the analytical solution of the equation can be derived as follows:

$$C(x,t) = C_0 + (C_p - C_0)erfc(\frac{x}{2\sqrt{Dt}}) \quad (4)$$

2.2.2. The second boundary condition

According to Fick's diffusion law, initial conditions, and the third boundary condition, the equation can be formed as [4],

$$\begin{cases} \frac{\partial C}{\partial t} = D\frac{\partial^2 C}{\partial x^2} & x > 0, t > 0 \\ C(x,0) = C_0 & 0 \le x < \infty,\ t = 0 \\ D\left(\frac{\partial C}{\partial x}\right)_{x=0} = \beta(C_s - C_p) & x = 0, t > 0 \end{cases} \quad (5)$$

According to equation (5), the analytical solution of the equation can be derived as follows:

$$C(x,t) = C_0 + (C_p - C_0)\left[erfc(\frac{x}{2\sqrt{Dt}}) - \exp\left(\frac{\beta x - \beta^2 t}{D}\right).erfc(\frac{x}{2\sqrt{Dt}} + \beta\sqrt{\frac{t}{D}})\right] \quad (6)$$

2.2.3. The combination of first, and third boundary conditions

According to Fick's diffusion law, initial conditions and the combination of first and third boundary conditions, the equation can be formed as [4],

$$\begin{cases} \frac{\partial C}{\partial t} = D\frac{\partial^2 C}{\partial x^2} & x > 0, t > 0 \\ C(x,0) = C_0 & 0 \le x < \infty,\ t = 0 \\ C_s = C(0,t) = C_p & x = 0, 0 < t < \infty \\ D\left(\frac{\partial C}{\partial x}\right)_{x=0} = \beta(C_s - C_p) & x = 0, t > 0 \end{cases} \quad (7)$$

According to equation (7), the analytical solution of the equation can be derived as follows,

$$C(x,t) = C_0 + (C_p - C_0)\frac{A\sqrt{t}}{1+A\sqrt{t}}erfc(\frac{x}{2\sqrt{Dt}}) \quad (8)$$

In the equation, $A = \beta$sqrt(π/D).

2.3. The optimization of MLR to mechanism model

2.3.1. The multivariate linear regression

Linear regression explores the linear changes of the dependent variables with the change of the independent variables. Multivariate linear regression (MLR) is to explore the changes of dependent variables when multiple influencing factors exist as independent variables. Assuming y is the dependent variable of MLR, and $[x_1, x_2, x_3 \cdots\cdots, x_n]$ are the independent variables of MLR, the MLR is written as follows equation [9],

$$y_i = b_0 + b_1 x_{1i} + b_2 x_{2i} + b_3 x_{3i} \cdots\cdots b_n x_{ni} + \mu \tag{9}$$

transfer the equation (10) into matrix form,

$$\begin{bmatrix} y_1 \\ y_2 \\ y_3 \\ \vdots \\ y_i \end{bmatrix} = \begin{bmatrix} 1 & x_{11} & \cdots & x_{n1} \\ 1 & x_{12} & \cdots & x_{n2} \\ 1 & x_{13} & \cdots & x_{n3} \\ \vdots & \vdots & \cdots & \vdots \\ 1 & x_{1i} & \cdots & x_{ni} \end{bmatrix} \begin{bmatrix} b_0 \\ b_1 \\ b_2 \\ \vdots \\ b_n \end{bmatrix} + \begin{bmatrix} \mu_0 \\ \mu_1 \\ \mu_2 \\ \vdots \\ \mu_n \end{bmatrix} \tag{10}$$

to simplify the equation (11),

$$Y = Xb \tag{11}$$

The coefficient $\hat{b}$ can be estimated by the ordinary least square method,

$$\hat{b} = (X'X)^{-1}X'Y \tag{12}$$

Then the estimated value of the dependent variable $\hat{Y}$ can be obtained as the following equation:

$$\hat{Y} = X\hat{b} \tag{13}$$

2.3.2. The optimization of the mechanism model

The optimization of MLR to carburizing mechanism model includes 7 steps, as shown in Fig.3,

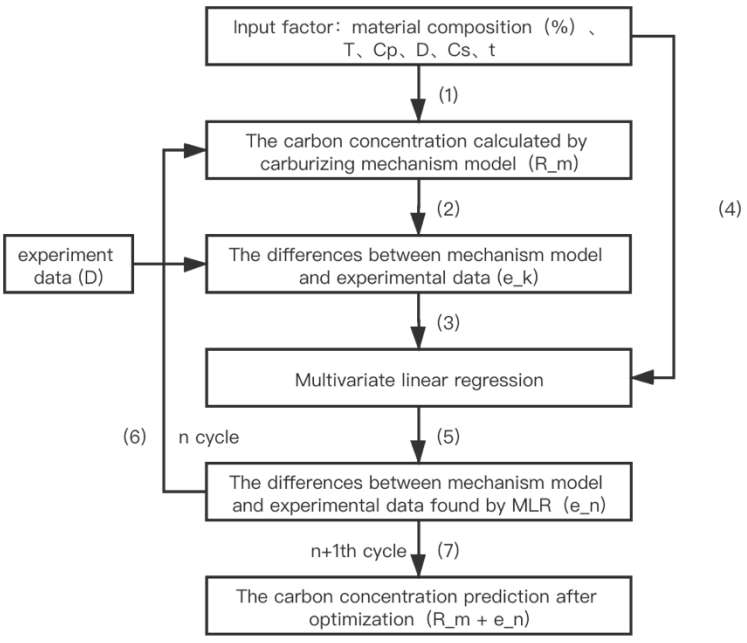

Figure 3: The optimization of MLR to mechanism model.

(1) Set the initial conditions and the factors of the model (which are the same as the independent variables of the MLR). Import those values into the mechanism model of carburizing process, then the carbon concentrations (R_m) of the workpiece at the different depths to the surface are found.

(2) Find the difference values e_k between the experimental results and results found by the mechanism model.

(3) Import the difference values e_k into the equation [12] as the dependent variable of MLR (the parameter Y).

(4) The input factors of the carburizing process are imported into the equation [12] as the parameter X, then the model coefficients $\hat{b}$ are found.

(5) The predicted difference values e_n between the experimental results and carburizing process mechanism model are found by MLR, which is the parameter $\hat{Y}$ in the equation [13].

(6) Add e_n to R_m found in step (1), then repeat step (2) to (5) n times. In this research, a total of 9 sets of experimental sample data are used for machine learning, thus the value of n is 9.

(7) Until finishing the 9th recycle, the final results are obtained. The values of the results are $R_m + e_n$. The physical meaning of the results is carbon concentrations (vol%) of samples predicted by the new model at different depths to the surface.

2.4. Relative Error

To find the difference between the predicted results and the experimental results, the relative errors should be calculated. In this experiment, the experimental results are provided as the exact solution, and the model predicted results are provided as the error solution. The calculation method of relative error is shown in the formula [14]. With the smaller relative error values, the results are more accurate.

$$R_e = \left|\frac{a-b}{a}\right| \tag{14}$$

In this equation, a is the experimental results, and b is the predicted results.

3. Discuss

To simplify the experiment process, all the experiment were performed when t = 8, x = 0.7, CP = 1.2%. When the surface carbon potential is 1.2% and the heating time is 8 hours, the carbon concentration in the workpiece is at 0.7mm depth to the surface of the workpiece.

Figure 4 shows the experimental results of the experimental samples. The x-axis is the sample number of the material used (see Appendix A for details), and the y-axis is the percentage of carbon concentration (vol%) in the current position.

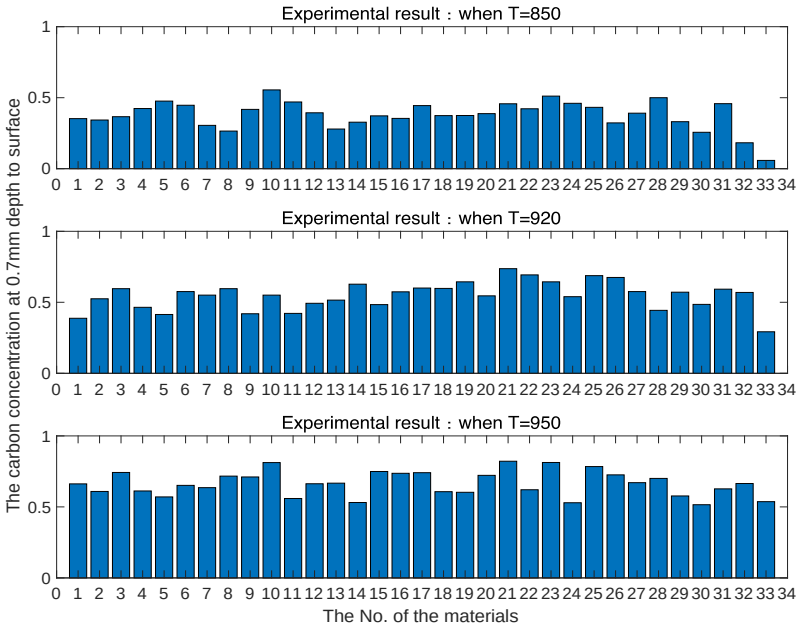

Figure 4: Experimental results

3.1. The results found by the mechanism model

Figure 5 shows the comparison between the mechanism model results and the experimental results. The x-axis is the sample numbers of the material used (see Appendix A for details), and the y-axis is the percentage of carbon concentration at the current position (vol%).

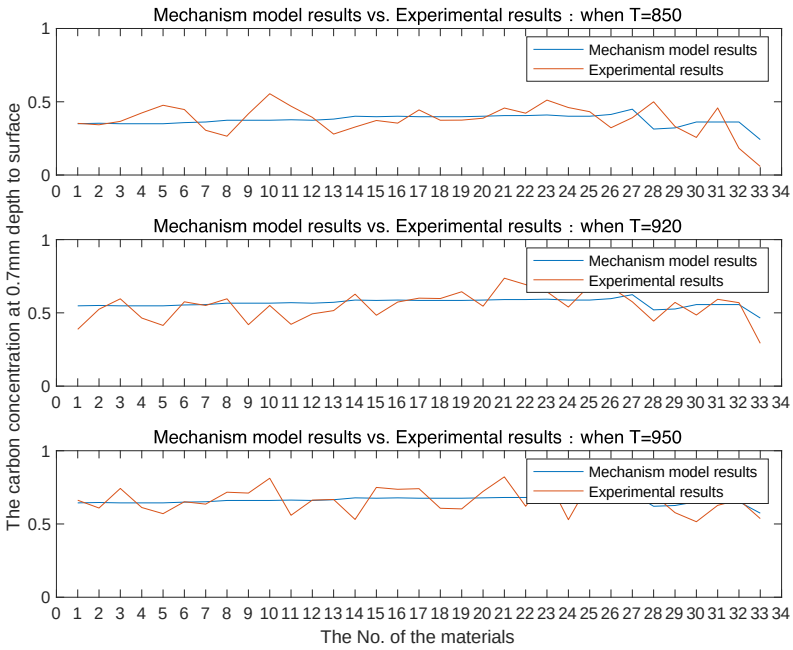

Figure 5: Mechanism model results vs. Experimental results

According to fig. 5, it can be observed that the trend of the simulation results and the experimental results is similar, but the error between the model results and the experimental results is large, especially the samples No. 10, No. 17, No. 28, etc. Samples No. 10, 17, and 28 are 16MnCrS5, 20MnCr5, and 9SMn28, which are all made of Mn (manganese). The main characteristic of the

manganese-based alloy is keeping the austenite formed from high temperature to room temperature with a stable stance, however, it will increase the time needed to form austenite [10]. The diffusion coefficient calculated by equation (2) of the mechanism model is based on the diffusion constant of the metal in the austenite stage. When below 900 ℃, the austenite has not been formed from some materials, thus the errors of the mechanism model results are large.

Meanwhile, Table 2 shows that with the increase in temperature, the error value can be significantly reduced. High temperature improves the transformation rate to austenite in metal [11], which effectively increases the accuracy of mechanism model simulation results. It can be seen that the low temperature (below 900 ℃) causes large errors in the mechanism model.

Table 2: Relative errors in different temperature

Temperature (℃)	850	920	950
Relative error	0.28	0.14	0.1

3.2. The results optimized by MLR

Fig. 6 shows the comparison between the results optimized by MLR and the experimental results. The x-axis is the sample numbers of the material used, and the y-axis is the percentage of carbon concentration at the current position (vol%).

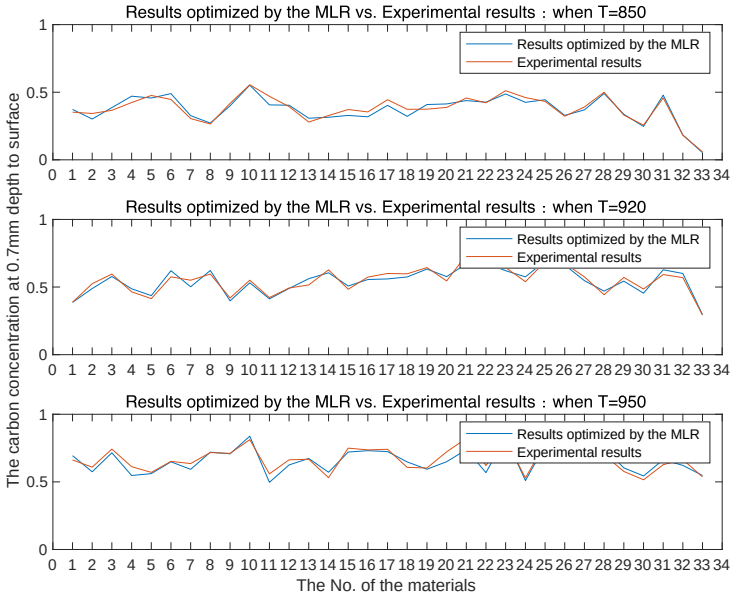

Figure 6: Results optimized by the MLR vs. Experimental results

From Figure 6, the results improved by introducing the MLR. Compared with the results obtained by using the mechanism model alone, the trends of optimized simulation results are closer to the experimental results. The relative errors of the MLR optimized model are shown in Table 3.

Table 3: Results optimized by the MLR in different temperature

Temperature (℃)	850	920	950
Relative error	0.0606	0.0456	0.0479

In addition, because of the self-learning ability of machine learning, with the increase in data sources, the predicted results should be more accurate with the increase in the cycle times. To verify the relative error value reduced by machine learning through the self-learning function, figure 7 shows the predicted results and the relative error values at the 1st, 3rd, 6th, 8th, and 9th cycle times.

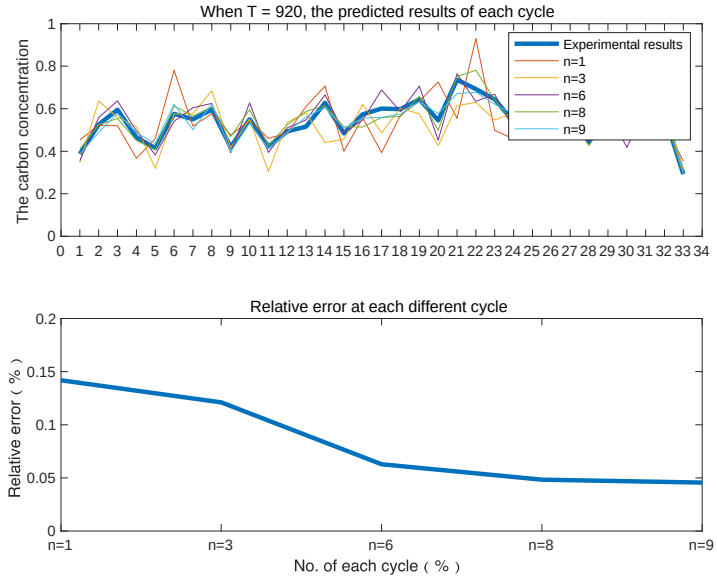

Figure 7: Results optimized and Relative error vs. recycle times

It can be seen from figure 7 that with the increase of the data set, the number of cycles in the model increases, and the relative error values can be effectively reduced. This indicated that by accumulating more data, the predicted results of the model are closer to the experimental results. Therefore, data accumulation has a positive effect on the optimization of the model.

4. Conclusion

In this paper, a method to optimize the carburizing process mechanism model using a multivariate linear regression model is proposed. Through experiments, the method is proven that it has a positive effect on improving the accuracy of predicted results. The characteristics of this method are as follow:

(1) The model is obtained by optimizing the mechanism model of carburizing process. Compared to machine learning alone, fewer data samples are needed to achieve practical application.

(2) With the increase of data, the model can significantly improve the accuracy of the results. The author of this paper will import this model into a web application, in which every user can upload more data for the model to further reduce the error value.

(3) The model has no limitations on materials, and carbonizing process of all kinds of metal materials can be improved by this method. However, the effect of this method on different furnaces has not been verified by experiments. In the future, the author will perform relevant experiments on different furnaces through follow-up topics and projects.

References

[1] S. Román, B. Ledesma, A. Álvarez, et al. Suitability of hydrothermal carbonization to convert water hyacinth to added-value products [J]. Renewable Energy, 146 (2004).

[2] Hilda Susan. The technology of the Heat Treatment of Steel: [J]. Journal of the Institution of Locomotive Engineers, 35(183), (2006).

[3] M. David, A. Khaled, R. Mark, S. John. Surface processing to improve the fatigue resistance of advanced bar steels for automotive applications. Materials Research Bulletin. (2005).

[4] V. S. Sagaradze. Effects of carbon content on the strength of carburized steel [J]. Metal Science and Heat Treatment, 3 (1970).

[5] S. Lee, D. Matlock, C. Tyne. Comparison of two finite element simulation codes used to model the carburizing of steel [J]. Computational Materials Science. (2013).

[6] A. Sugianto, M. Narazaki, M. Kogawara, A. Shirayori, S. Kim, S. Kubota. Numerical simulation and experimental

verification of carburizing-quenching process of SCr420H steel helical gear [J]. Journal of Materials Processing Tech. 7 (2008).
[7] H. Chen, Z. Sybrand. Predicting the Effect of Mo, Ni, and Si on the Bainitic Stasis [J]. Metallurgical and Materials Transactions. 8 (2014).
[8] Roderick Lucas and Laurel Dalton. Machine learning and applications; proceedings. [J]. SciTech Book News, 32 (2008).
[9] Ethel Carrie. Linear regression analysis; theory and computing. [J]. SciTech Book News, 33 (2009).
[10] E. Gamsjger, H. Chen, S. Zwaag. Application of the cyclic phase transformation concept for determining the effective austenite/ferrite interface mobility [J]. Computational Materials Science. (2014).
[11] V. S. Sagaradze. Effects of carbon content on the strength of carburized steel [J]. Metal Science and Heat Treatment. 3 (1970).

Appendix A

No.	Materials	%C	%Si	%Mn	%Cr	%Ni	%Mo	%N	%AI	%V	%Cu	%P	%S	%T
1	13 NiCr 6	0.135	0.250	0.400	0.750	1.425	0.000	0.000	0.000	0.000	0.000	0.025	0.025	0.000
2	14 Ni 6	0.140	0.225	0.450	0.000	1.450	0.000	0.000	0.000	0.000	0.000	0.025	0.025	0.000
3	14 NiCr 10	0.135	0.250	0.550	0.750	2.500	0.000	0.000	0.000	0.000	0.000	0.025	0.025	0.000
4	14 NiCr 14	0.135	0.250	0.550	0.750	3.500	0.000	0.000	0.000	0.000	0.000	0.025	0.025	0.000
5	14 NiCr 18	0.135	0.250	0.550	1.100	4.500	0.000	0.000	0.000	0.000	0.000	0.025	0.025	0.000
6	15 CrNi 6	0.145	0.275	0.500	1.550	1.550	0.000	0.000	0.000	0.000	0.000	0.025	0.025	0.000
7	15 NiCr 6 4	1.500	0.250	0.800	1.090	1.450	0.000	0.000	0.000	0.000	0.000	0.000	0.000	0.000
8	16 CrMo 4	0.165	0.250	0.650	1.050	0.300	0.250	0.000	0.000	0.000	0.000	0.250	0.250	0.000
9	16 MnCr 5	0.165	0.275	1.150	0.950	0.000	0.000	0.000	0.000	0.000	0.000	0.025	0.025	0.000
10	16 MnCrS 5	0.165	0.275	1.150	0.950	0.000	0.000	0.000	0.000	0.000	0.000	0.025	0.025	0.000
11	17 Cr 3	0.170	0.275	0.550	0.750	0.000	0.000	0.000	0.000	0.000	0.000	0.025	0.025	0.000
12	17 CrNiMo 6	0.165	0.275	0.500	1.650	1.550	3.000	0.000	0.000	0.000	0.000	0.025	0.025	0.000
13	18 CrNi 8	0.175	0.275	0.500	1.950	1.950	0.000	0.000	0.000	0.000	0.000	0.025	0.025	0.000
14	20 Cr 4	0.200	0.300	0.750	1.050	0.000	0.000	0.000	0.000	0.000	0.000	0.025	0.025	0.000
15	20 CrMoS 4	0.195	0.275	0.750	0.400	0.000	0.450	0.000	0.000	0.000	0.000	0.025	0.025	0.000
16	20 CrS 4	0.200	0.300	0.750	1.050	0.000	0.000	0.000	0.000	0.000	0.000	0.025	0.025	0.000
17	20 MnCr 5	0.195	0.275	1.250	1.150	0.000	0.000	0.000	0.000	0.000	0.000	0.025	0.025	0.000
18	20 MnCrS 5	0.195	0.275	0.125	1.150	0.000	0.000	0.000	0.000	0.000	0.000	0.025	0.028	0.000
19	20 MnCr 4	0.195	0.275	0.750	0.400	0.000	0.450	0.000	0.000	0.000	0.000	0.025	0.025	0.000
20	20 CrMnMo	0.200	0.270	1.050	1.250	0.000	0.250	0.000	0.000	0.000	0.000	0.000	0.000	0.000
21	20 CrMnTi	0.205	0.270	0.950	1.150	0.000	0.000	0.000	0.000	0.000	0.000	0.000	0.000	0.070
22	20 CrMo	0.205	0.270	0.550	0.950	0.000	0.200	0.000	0.000	0.000	0.000	0.000	0.000	0.000
23	21 MnCr 5	0.210	0.250	1.250	1.150	0.000	0.000	0.000	0.000	0.000	0.000	0.025	0.000	0.000
24	21 NiCrMo 2	0.200	0.275	0.750	0.500	0.550	0.200	0.000	0.000	0.000	0.000	0.025	0.025	0.000
25	21 NiCrMoS	0.200	0.300	0.800	0.550	0.550	0.200	0.000	0.000	0.000	0.000	0.250	0.028	0.000
26	22 CrMoS 3 5	0.215	0.300	0.850	0.850	0.000	0.450	0.000	0.000	0.000	0.000	0.025	0.028	0.000
27	25 MoCrS 4	0.260	0.275	0.750	0.500	0.000	0.450	0.000	0.000	0.000	0.000	0.025	0.280	0.000
28	9 SMn28	0.090	0.030	1.100	0.000	0.000	0.000	0.000	0.000	0.000	0.000	0.060	0.280	0.000
29	C 10	0.100	0.250	0.450	0.000	0.000	0.000	0.000	0.000	0.000	0.000	0.025	0.025	0.000
20	C 15	0.150	0.250	0.450	0.000	0.000	0.000	0.000	0.000	0.000	0.000	0.025	0.025	0.000
31	Ck 15	0.150	0.250	0.450	0.000	0.000	0.000	0.000	0.000	0.000	0.000	0.025	0.025	0.000
32	Cm 15	0.150	0.250	0.450	0.000	0.000	0.000	0.000	0.000	0.000	0.000	0.025	0.028	0.000
33	Fe	0.000	0.000	0.000	0.000	0.000	0.000	0.000	0.000	0.000	0.000	0.000	0.000	0.000